Permanent CO$_2$ Sequestration in Ocean Sediments: Flow-Through Reactor Studies

March 2011

nyserda

Energy. Innovation. Solutions.

nyserda
Energy. Innovation. Solutions.

The New York State Energy Research and Development Authority (NYSERDA) is a public benefit corporation created in 1975 by the New York State Legislature.

NYSERDA derives its revenues from an annual assessment levied against sales by New York's electric and gas utilities, from public benefit charges paid by New York rate payers, from voluntary annual contributions by the New York Power Authority and the Long Island Power Authority, and from limited corporate funds.

NYSERDA works with businesses, schools, and municipalities to identify existing technologies and equipment to reduce their energy costs. Its responsibilities include:

- Conducting a multifaceted energy and environmental research and development program to meet New York State's diverse economic needs.

- The New York Energy $martSM program provides energy efficiency services, including those directed at the low-income sector, research and development, and environmental protection activities.

- Making energy more affordable for residential and low-income households.

- Helping industries, schools, hospitals, municipalities, not-for-profits, and the residential sector, implement energy-efficiency measures. NYSERDA research projects help the State's businesses and municipalities with their energy and environmental problems.

- Providing objective, credible, and useful energy analysis and planning to guide decisions made by major energy stakeholders in the private and public sectors.

- Since 1990, NYSERDA has developed and brought into use successful innovative, energy-efficient, and environmentally beneficial products, processes, and services.

- Managing the Western New York Nuclear Service Center at West Valley, including: overseeing the State's interests and share of costs at the West Valley Demonstration Project, a federal/State radioactive waste clean-up effort, and managing wastes and maintaining facilities at the shut-down State-Licensed Disposal Area.

- Coordinating the State's activities on energy emergencies and nuclear regulatory matters, and monitoring low-level radioactive waste generation and management in the State.

- Financing energy-related projects, reducing costs for ratepayers.

For more information, contact the Communications unit, NYSERDA, 17 Columbia Circle, Albany, New York 12203-6399; toll-free 1-866-NYSERDA, locally (518) 862-1090, ext. 3250; or on the web at www.nyserda.org

STATE OF NEW YORK
Andrew M. Cuomo, Governor

ENERGY RESEARCH AND DEVELOPMENT AUTHORITY
Vincent A. DeIorio, Esq., Chairman
Francis J. Murray, Jr., President and Chief Executive Officer

PERMANENT CO₂ SEQUESTRATION IN OCEAN SEDIMENTS:
FLOW-THROUGH REACTOR STUDIES

Final Report

Prepared by:
LAMONT-DOHERTY EARTH OBSERVATORY
Palisades, NY

David Goldberg
Juerg Matter

Abstract

A popular approach to avoid to anthropogenic carbon dioxide release to the atmosphere involves geologic carbon sequestration - the injection of CO2 into rocks and sediments beneath the land surface or below the seafloor. This project investigated CO2 storage in reservoir rocks and deep ocean sediments by conducting two laboratory-scale experiments: 1) using proxy materials to observe hydraulic fracturing and geomechanical behaviors of sub-ocean sediments in the absence of a caprock; and 2) using a core flooding reactor capable of replicating in situ conditions to measure multi-phase flow properties of typical reservoir rocks. Proxy experiments suggest that conventional petroleum engineering methods applied to deep-ocean sediment injection would likely be complex, and potentially risky. Core flooding experiments indicate that the relative permeability of injected CO2 replacing brine in reservoir samples ranged between 0.35-0.4. These values indicate that CO2 does not behave as an inert non-wetting fluid, but rather as a weakly, or intermediate, water-wetting phase. Based on this observation, CO2 injectivity in geological reservoirs will be reduced, and pressure-limited reservoirs will have reduced storage capacity. Thus, modelling efforts should incorporate the measured relative permeability of each specific formation to evaluate capacity. Assuming these findings apply broadly, approximately twice the reservoir volume and related infrastructure would be required to store a given amount of CO2 below the surface of the Earth.

Notice

Keywords

Contact Information

David Goldberg, Lamont-Doherty Earth Observatory, Borehole Research, Palisades, NY 10964
Phone: 845-365-8674; email: goldberg@ldeo.columbia.edu

Juerg Matter, Lamont-Doherty Earth Observatory, 205 Comer, Palisades, NY 10964
Phone: 845-365-8543; email: jmatter@ldeo.columbia.edu

Table of Contents

Executive Summary

Laboratory experiments have been performed to analyze the feasibility of carbon dioxide disposal in ocean sediments, where liquid CO_2 would potentially be injected into permeable formations. The injection of liquid CO_2 into ocean sediments requires knowledge of the geomechanical behavior of these formations, the behavior of the CO_2 after injection, the long-term fate of CO_2-water-rock reactions, and the role of CO_2 hydrates. A set of experiments was designed to address these issues. Geomechanical proxy experiments and CO_2 flow-through experiments were conducted. The reactivity of CO_2-water-rock mixtures and hydrate experiments were not completed due the complexity and importance of the results from the fundamental flow-through experiments, but experimental capability and expertise were developed to conduct such follow-on experiments in the future.

Fundamental results from the geomechanical proxy experiments determined that fracturing instabilities must be resolved to enable injection in ocean sediments, such as those found off the coast of the northeastern United States. Results from the flow-through reactor experiments determined that the critical parameter for CO_2 injection into water-saturated formations – the relative permeability – is a factor of two or more lower than previously anticipated. This result indicates that CO_2-water interactions are much more important than previously thought and will impact the reservoir capacity for CO_2 storage in ocean sediment reservoirs as well as in other geological storage reservoirs, affecting both the volume capacity and pressure in a potential storage reservoir.

I. Introduction and Motivation

Anthropogenic carbon dioxide emissions to the atmosphere are the primary source of anthropogenic global warming and ocean acidification, and as such must be avoided (IPCC, 2007). Geologic carbon sequestration, the injection of CO_2 emissions into rock formations, has been proposed as a possible solution (IPCC, 2005). Carbon dioxide injection into ocean sediments below 2700 m water depth and a few hundred meters of sediments may provide permanent geologic storage by gravitational trapping and CO_2 hydrate formation (House et al., 2006). At high pressures and low temperatures common in deep sea sediments a few hundred meters below sea floor, CO_2 will be in its liquid phase and will be denser than the overlying pore fluid. The lower density of the pore fluid provides a cap to the denser CO_2 and ensures gravitational trapping. Dissemination of the injected CO_2 in the sediments and potential chemical reactions between CO_2, pore fluid, and sediments will define its fate in the storage reservoir. The overall goal of the project is to design experiments in the laboratory to demonstrate the viability of CO_2 storage in ocean sediments.

The storage capacity of ocean sediments is potentially large, many times current annual CO_2 emissions (Bielicki, 2007). The large scale of potential gravitational sequestration in deep ocean sediments and the proximity to densely populated coastal areas near the edge of the continental shelf make this an attractive possibility for CO_2 sequestration. However, Levine et al. (2007) presented data showing that the dominant pelagic calcareous and clay lithologies at the necessary seafloor depths have very low permeabilities, on the order of microdarcies to nanodarcies, challenging the practicality of significant CO_2 injection into these formations. Hydraulic fracturing has allowed industry to economically produce gas from shales with similar permeabilities (see, e.g., Parshall, 2008), however, suggesting that hydraulic fracturing may enable CO_2 sequestration at such low permeabilities.

For hydraulic fracturing to be a viable reservoir upgrading technique, fractures must be stable and must not provide a conduit from the wellbore to the seafloor and open ocean above. In the deep ocean, sediments are horizontally isotropic and primarily stressed from overburden weight alone such that horizontal stresses originate from a zero strain condition. Because hydraulic fractures propagate perpendicular to the minimum stress, and horizontal stresses are smaller than the vertical stress, fractures will be oriented vertically. However, in the deep ocean, the absence of a mechanical seal (caprock) at the seafloor presents a risk that hydraulic fractures

will propagate to the open ocean (Levine et al., 2007). Furthermore, without a mechanical seal any vertical accumulation of liquid CO_2 at depth may buoyantly push up through the denser overlying weak sediments and propel itself to the seafloor (Levine et al., 2007). These fracturing-induced mechanical instabilities must be overcome to be able to take advantage of the potential benefits of gravitational sequestration in deep ocean sediments.

It is important to know how much CO_2 can be disposed of in a given reservoir, both onshore and offshore, for capacity estimation and source-sink matching. It is equally important that there is minimal, if any, leakage of CO_2. Among many factors, the injection pressure is limited by the fracturing pressure of the caprock, its capillary breakthrough pressure, and the extent of CO_2 plume migration. To determine both pressure rise and fluid migration requires reservoir-scale modeling incorporating multiphase physics of CO_2 injection into water-filled reservoirs. Laboratory-scale experiments are necessary to control critical input parameters such as the relative permeability of CO_2 in water-wet formations and the geomechanical properties of ocean sediments. We designed and conducted two different sets of experiments, described below, to address these problems. Laboratory experiments were designed and conducted to simulate the geomechanical behavior of CO_2 injected into ocean sediments as well as the relative permeability of liquid CO_2 injected into water-laden reservoirs.

II. Geomechanical Experiments

Geomechanical experiments were conducted using transparent materials such as gelatin and transparent clay as proxies for weak, low-permeability deep ocean sediments. Experiments successfully replicated previous studies and indicate that fractures in deep ocean sediments will preferentially propagate vertically and upwards to the surface. Such fractures would create conduits for injected CO_2 to bypass the permeable sediments entirely and instead create direct paths from the injection wellbore to the surface. Vertical accumulations of injected fluids in fractures may also propagate through the weak sediments to the seafloor. Our experiments were able to replicate vertical and buoyant fracturing and fracture propagation, as well as testing various fracture arrest mechanisms.

The most promising fracture arrest mechanism was borrowed from petroleum reservoir engineering -- a buoyant impermeable material is injected that rises to the top of the fracture and prevents further vertical growth upwards. Buoyant fracture rise occurs when the minimum

effective stress gradient is greater than the hydrostatic pressure gradient within the fracture, i.e. a static difference, and so will not be affected by the use of a buoyant diverter that dynamically alters the local pressures. Injecting proppant (e.g., sand) into fractures could arrest buoyant fractures by providing a physical space for the pressurized fracture fluid to remain trapped without being squeezed upward by its own buoyancy. By using appropriate reservoir engineering techniques such as proppant, fracturing induced by geomechanical instabilities may be avoided and potentially allow for safe hydraulic fracturing in shallow marine sediments[1]

Materials and Methods

To study different fracturing and arresting mechanisms in the laboratory, we created a simple physical model capable as a proxy to test different potential instabilities. Gelatin has been used previously as a sediment proxy to study artificially induced fractures for oil drilled cuttings disposal as well as natural fracture systems (Bakala, 1997). Studies of the effect of state of stress on fracture orientation also used gelatin for the sediment or rock and plaster-of-Paris slurry as the fracturing fluid (Hubbert and Willis, 1957). Takada (1990) used gelatin to study propagation and propagation rates of buoyant hydraulic fractures. To study different failure modes, we used a rectangular acrylic container with a depth and width of 0.3 m (12") and height of 0.76 m (30"). This container was filled to about 0.5 m with gelatin prepared by mixing 2% weight Type A gelatin (Great Lakes Gelatin, Grayslake IL) and water at a temperature of 60-70°C and then left in a refrigerator to solidify overnight. Various gelatin concentrations were tested, ranging from the 1.25% used by Takada (1990) to the 12% used by Hubbert and Willis (1957). The lowest values proved to be particularly weak: small perturbations caused separation of the gelatin from the injection pipe. Higher concentrations introduced greater strengths but created gelatin dispersal problems while gaining no particular advantage.

A 0.15 cm (1/16") inner diameter, 0.3 cm (1/8") outer diameter horizontal pipe positioned at 7.6 cm (3") height above the bottom of the rectangular box passing through the box was used to inject fluid from a cut at its mid-point. A metal rod was then inserted for gelatin formation, and upon removal provided a continuous path for the injected fluid to displace all the

---

[1] Results from our geomechanical proxy experiments were presented in a conference paper, "Gravitational trapping of carbon dioxide in deep sea sediments: Permeability upgrading and mechanical stability," at the 9th International Conference on Greenhouse Gas Control Technologies (GHGT-9), and published in *Energy Procedia* (Levine et al. 2011).

air in the tube before the start of fracturing. Fracturing in the gelatin was initiated once all the air was displaced from the pipe and reproduced vertical buoyant migration of fractures (Takada, 1990). A variety of materials were used as injection fluids; dyes (food coloring, oil red) were mixed into all injection fluids to enable easier visualization and recording with standard photographic equipment.

Results

We were able to produce vertical fracture propagation and buoyant fractures using vegetable oil, mineral oil, and linseed oil as the injection fluids; a stationary fracture using water; and a sinking fracture using glycerin. Ethanol produced an unusual interaction with the gelatin at the well outlet after initial rise, followed by fractures at steeply dipping angles downwards despite its low specific density (0.79 g/cc). To test tensile strength, experiments were run with a fracture created by connecting the injection well to tubing taped along the side of the acrylic box with the liquid level slightly higher than the gelatin level. Fracturing could be stopped and started and the fracture emptied or filled by changing the height of the tubing containing the fracturing fluid. Fracturing was found to commence at about 3 cm above the gelatin in 1.6 mm (1/16") inner diameter plastic tubing and about 1.5 cm above the gelatin in 6.4 mm (1/4") inner diameter plastic tubing with water as the fracturing fluid. When heights are corrected for the capillary effect of the tubing, the hydraulic fracturing tensile strength is found to correspond to a hydraulic head of about 1 cm, consistent with the ~10^2 Pa tensile strength reported from a bending test (Takada, 1990). Fracture filling with the same capillary corrections was nearly identical to the gelatin height, confirming previous results that gelatin is hydrostatically stressed and isotropic (Takada, 1990).

The relative homogeneity of pelagic sediments makes large discontinuities or changes in stiffness unlikely. Gudmundsson and Brenner (2001) suggest that discontinuities, changes in stiffness between layers, and stress barriers may each contribute to fracture arrest. While natural stress barriers are not expected in ocean sediments, Warpinski and Branagan (1989) show that stress alteration due to hydraulic fracturing changes the direction of minimum in-situ stress and can cause a subsequent fracture to open in a different direction. Hydraulic fracturing may therefore be used to create stress barriers or to change fracture orientations -- two possibilities that can be tested using the gelatin model. An artificial stress barrier might be created by a

hydraulic fracture in an upper layer to prevent a fracture in a lower layer from extending upwards (Warpinski and Branagan, 1989). Fracture orientation in this case changes by altering the stress field in both horizontal directions, making the minimum in-situ stress vertical, and thus the induced fracture propagates horizontally. In one gelatin experiment, we placed a 15 cm (6") layer of sand on top, creating a stress barrier that arrested a buoyant vegetable oil fracture (Figure 1a) and prevented vertical fracture propagation from the injection well (Figure 1b). Instead, the induced fracture propagated laterally (Figures 1c, 1d). When the overburden weight of the sand was preferentially loaded on top of the gelatin, causing it to compress against the bounding wall, the induced fracture could not push through the overlying compressed layer and connect with the higher permeability sand above (Figure 1e, f).
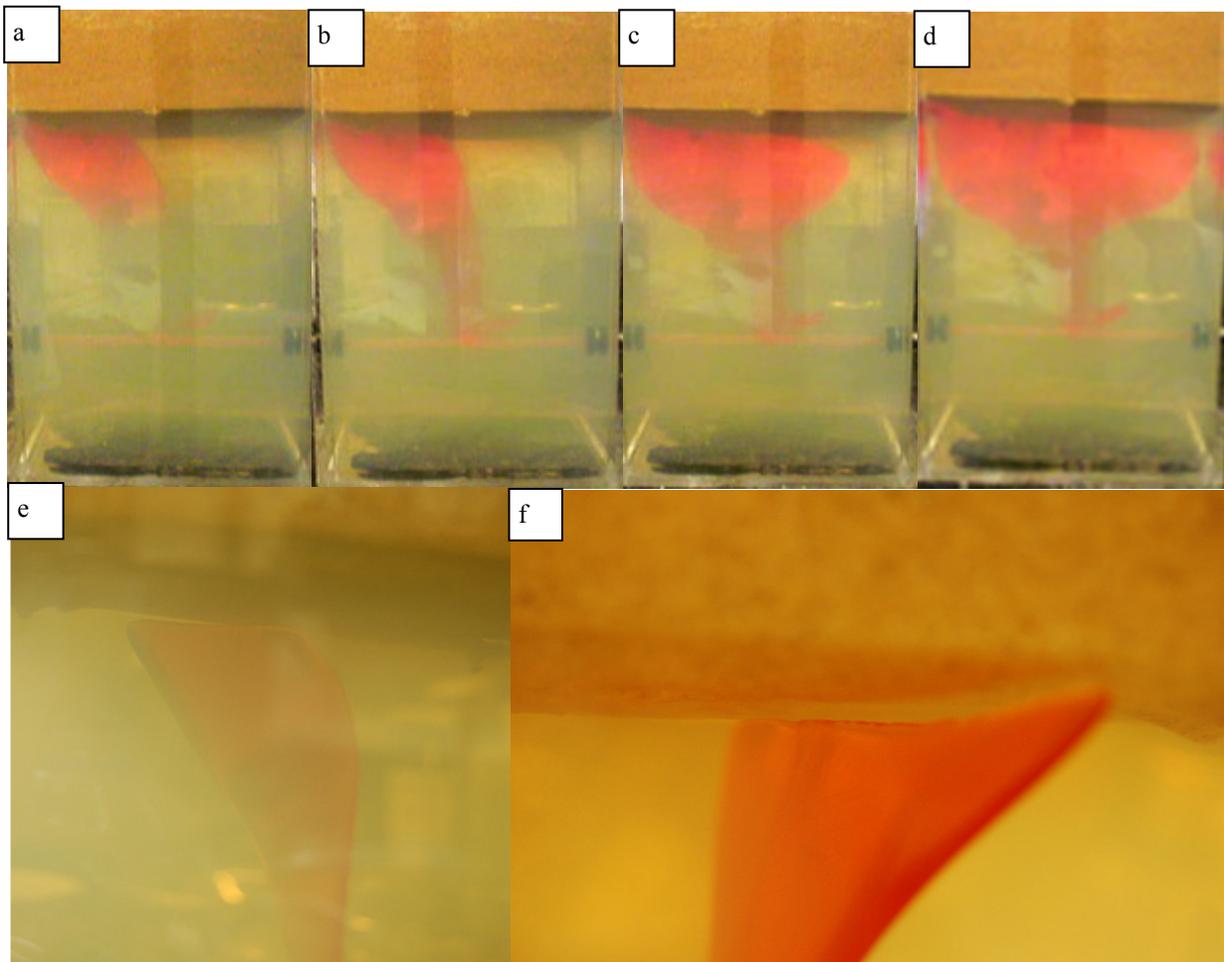
Figure 1: Stress barrier arresting fracture growth. Figure 1a-d top left to right: The weight of the sand creates a stress barrier in the uppermost layer of gelatin causing, (1a) a buoyant vegetable fracture to stop rising, (1b) preventing pressurized vertical propagation, (1c,d) and lateral fracture propagation; 1e,f bottom left and right: The fracture cannot push through the gelatin immediately below the sand and does not meet the sand layer above.

Discussion

With the ability to reproduce and visualize hydraulic fracturing and buoyant fracture rise using transparent gelatin, laponite, and dyed fluids, we are able to consider different reservoir engineering solutions for arresting vertical fracture growth and buoyant fracture.

A possible reservoir engineering technique for injecting into a formation without a stress barrier is to inject a buoyant material that rises to the top of the fracture and causes a local reduction in permeability (Nguyen and Larson, 1983). This causes a large pressure drop at the fracture tip that diverts the fracture from growing upward (Nguyen and Larson, 1983). By lowering the pressure at the upper fracture tip but not at the other fracture tips, the fracture can still expand laterally, or downward, but has insufficient pressure at the top of the fracture to continue propagating upwards. Relying on a buoyant diverter for vertical fracture stabilization requires that any lateral extension of a fracture must be accompanied by successful diverter placement at the top of the fracture to avoid the fracture "mushrooming" beyond the barrier (Barree and Mukherjee, 1995). Using a buoyant diverter is a dynamic method of preventing fracture extension upwards. It works because the flowing fracture fluid loses pressure while pushing through the impermeable diverter. Hydraulic fractures kept open by injection pressure buoyantly rise if the minimum effective stress gradient is greater than the hydrostatic pressure gradient within the fracture (Secor and Pollard, 1975; Simonson et al., 1978). A buoyant diverter may therefore stem fracture runaway to the seafloor, but would not affect buoyant fractures that rise from static differences in pressure gradients. Secor and Pollard (1975) presented a theoretical model of open fracture buoyant instability and concluded that proppant (i.e., sand) could be used to prevent buoyant propagation by "reducing the operating pressure" (i.e., lose pressure and close around a proppant). Upon fracture closure, contained fluids and proppant can no longer contribute to buoyant fracturing; therefore, injecting proppant into fractures may prevent buoyant fracture rise. Injecting a buoyant diverter or sand proppant into an unstable fracture in gelatin would test this arrest mechanism.

III. Flow-Through Reactor Experiments

We conducted a set of relative permeability experiments with CO_2 displacing water in both natural and artificial cores. The experiments were designed in such a way to obtain only the relative permeability of CO_2 displacing water at residual water saturation -- the so called

"drainage end point" relative permeability. While this state only corresponds to conditions typically found immediately adjacent to an injection well, it provides a deeper, more important piece of information: the comparative in-situ wettability of CO_2 and water, providing the critical relative permeability curve.

A flow-through experimental system was designed, built, tested, and operated at Schlumberger-Doll Research in Cambridge, MA. Schlumberger provided material and personnel support for the components and construction of the laboratory apparatus. The system pushes high-pressure liquid CO_2 through water-filled rocks at conditions that are similar to those found in ocean sediments. Initial experiments were performed to measure transport properties of CO_2 and, in particular, CO_2/brine relative permeability experiments under characteristic reservoir conditions.

Background: Multiphase Flow in Porous Media

This background section presents an overview of the motivation and basic physics necessary to understand the flow-through experimental system design and results. Multiphase flow in porous media is controlled by a combination of Darcy's Law type viscous forces and capillary forces. While Darcy's Law modified for multiphase flow (Equation 1) controls bulk flow and pressure, it is the capillary pressure drop at pore throats that determines pore occupancy according to the Young-Laplace equation (Equation 2).

$$Q/A = v = (kr\ k\ /ì)\nabla P \qquad\qquad\qquad (Eq.\ 1)$$

$$Pc = Pnw - Pw = 2\sigma\ cos\theta/R \qquad\qquad\qquad (Eq.\ 2)$$

Variables are defined as: Q: volumetric flow rate; A: area; v: fluid velocity; k: intrinsic permeability; ì: viscosity; ∇P: pressure gradient, which for a core is equal to the pressure drop ÄP across the core length L, $\nabla P = ÄP/L$; P_c: capillary pressure; P_{nw}: non-wetting phase pressure; P_w: wetting phase pressure; σ: interfacial surface tension between the two fluid phases; θ: contact angle; and R: pore throat radius. k_r is defined as the relative permeability, the percentage of intrinsic permeability for a given phase due to blockage of finite flow pathways and varying between 0 and 100%.

Viscous pressure drop due to multiphase Darcy flow controls reservoir-scale flow and pressures, setting the pressure drop between phases at the pore-scale. Therefore, the pressure drop due to multiphase Darcy flow will determine capillary-controlled pore occupancy (see, e.g., Willhite, 1986). Liquid-liquid-rock surface forces determine the relative wettability of a rock for a pair of fluids. While a wetting fluid will fully spread across a surface, forming a continuous film, a non-wetting fluid will pull away from the surface and form individual beads or droplets. In a porous media, a wetting fluid will be pulled into the smallest pores first due to capillary surface forces, whereas a non-wetting fluid will be prevented from accessing the smallest pores due to capillary surface forces and will instead occupy the largest pores first. Capillary surface forces therefore control the occupancy of the largest and most permeable pathways, as well as the smallest and least permeable pathways (see, e.g., Willhite, 1986; Anderson, 1987).

At flow rates found in typical reservoirs, capillary forces prevent full displacement of the resident fluid by the invading fluid. An invading non-wetting fluid will, therefore, leave behind a residual wetting phase, while an invading wetting fluid will leave behind an irreducible non-wetting phase. In either case, the non-displaced resident fluid blocks flow pathways, thereby reducing the relative permeability. The relative permeability of an invading wetting phase is very low, typically around 0.1, because the resident non-wetting phase remains in the largest pores and blocks the most permeable pathways. The relative permeability of an invading non-wetting phase is very high, in the range of 0.8-1, because the resident wetting fluid only remains in the smallest pores, which contribute least to flow pathways. By measuring the relative permeability of CO_2 displacing water at the residual water saturation, we are able to experimentally test whether or not CO_2 behaves as an inert, non-wetting fluid.

While a wetting phase fluid will imbibe into the smallest pores of a rock saturated with non-wetting phase fluid, a non-wetting phase fluid requires a finite pressure to achieve a percolation threshold, the first flow path across a rock. Because capillary pressure elevation is inversely proportional to pore throat radius, the breakthrough pressure, P_b, is set by the largest pore throat radius, R_{max}, at which percolation occurs:

$$P_b = 2\sigma \cos\theta / R_{max} \qquad \text{(Eq. 3)}$$

Because pore occupancy is controlled by capillary forces, the ratio of the pressure drop at a given flow rate to the breakthrough pressure, $\Delta P/P_b$, corresponds to the ratio of the larger pore throat radius at breakthrough to the occupied pore throat radius at a given flow rate, R_{max}/R. The

distribution of pore throat radii are tightly clustered for the Berea sandstone and alumina ceramic P3C cores tested. Therefore high $\Delta P/P_b$ ratios ensure that residual water saturation is achieved. Furthermore, the capillary number, the ratio of viscous to capillary forces, is kept many orders of magnitude below the levels needed to mobilize residual water (Anderson, 1987).

Materials and Methods

The design of the laboratory system built at Schlumberger for these flow-through experiments is shown in Figure 2. This system pushes liquid or supercritical CO_2 (20 or 50°C, 100 bar) through a brine-saturated core sample at a series of constant flow rates while the pressure drop across the core is monitored. The fluid back pressure, temperature, and radial jacketing pressure are also controlled and monitored. A brief description of sample preparations and experimental runs are presented below.

High Pressure Core Flooding Reactor
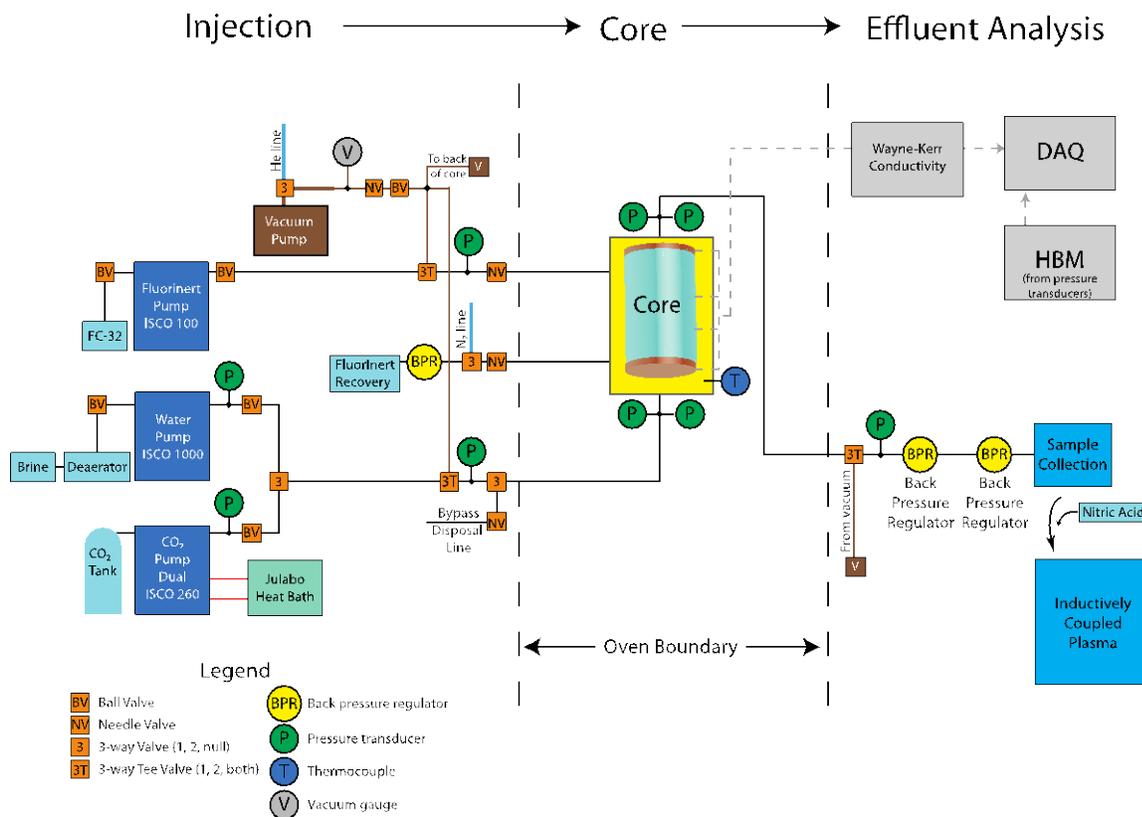
Figure 2: Schematic of the laboratory system design for flow-reactor experiments.

Sample preparation and apparatus

Several sample cores were tested under a variety of conditions, using this experimental apparatus. Rock cores included Berea sandstone, chosen for its relative homogeneity and the wealth of data available, and synthetic P3C alumina ceramic (CoorsTek), chosen to be homogeneous, isotropic, and nearly inert. Porosity measurements were made on 3.8 cm (1.5") by 3.8 cm (1.5") cores sampled adjacent to the experimental cores. Cores were prepared to be approximately 10 cm (4") in length and 3.8 cm (1.5") in diameter. Later experiments were conducted with P3C cores 20 cm (8") in length to ensure minimized end effects. All cores were vacuum-dried overnight at 70°C prior to each experiment.

During each experiment, cores were placed in a high-pressure Hassler-type core holder rated to 137 bar (2,000 psi Temco ECH series) held vertically in a custom-made stand. Cores were sealed in a rubber sleeve made of either Viton fitted with a pair of impedance terminals or Buna-N, used to transmit a radial jacketing pressure of 137 bars (2,000 psi) while preventing flow from bypassing around the sample. Radial pressure was applied with an electrically nonconductive fluorinert FC-40 (3M) by a syringe pump (Teledyne Isco 100DM) in constant pressure mode. A precision impedance analyzer (Wayne Kerr 6520B) was used to monitor impedance and phase angle. The core holder and pressure transducers were contained in a temperature-controlled chamber (Tenney TJ30S) with a rated accuracy of 0.3°C measured by an internal RTD. All tubing and fittings were Swagelok stainless steel 316L and were leak tested to < 10 nL/s with a He leak detector (Matheson Leak Hunter 8065). Prior to each experiment, an oil-free vacuum pump (Sahara 8350) was used to evacuate air from the system for 12-24 hours.

Fluid injection and measurement

Samples were initially flooded with brine consisting of 18.2 MΩ-cm water (Millipore Synergy UV) with 50,000 ppm (m/m) NaCl (Fisher Scientific ACS Grade) with 50 ppm (m/m) LiCl (Fisher Scientific ACS Grade) tracer to be used to test for salt precipitation. Later experiments with P3C alumina cores used deionized (DI) water and confirmed that salt precipitation did not significantly affect permeability measurements. Brine and DI water were loaded from a deaerator (Geokon The Nold) directly into an evacuated syringe pump (Teledyne Isco 1000D) under vacuum. For reference, brine was also sampled via a bypass line immediately before the core flood. CO_2 was dispensed at a constant flow rate from a paired set of syringe

pumps (Isco 260D) with an air valve package to minimize pressure transients at pump switchover. Liquid CO_2 was siphoned directly from a CO_2 cylinder (American Gas Products 99.8% bone dry). A recirculating temperature bath was used to control temperature in the syringe pumps via a fiberglass-insulated temperature jacket (Teledyne Isco) around each syringe pump barrel. In all cases, cores were held vertically to ensure flow was parallel to gravity. Initial experiments injected CO_2 into the core from below to align buoyancy and viscous instabilities; later experiments injected CO_2 from above to create a buoyancy-stabilized plume front. System pressure was controlled by two back-pressure regulators in series (Tescom 26-1700 series), with the first electronically controlled (Tescom ER3000) and the second manually set to approximately 5-10 bars less than the experimental pressure while the first regulator was fully opened. Effluent was sent to a sampling system consisting of 20 high-pressure 40 mL sampling containers (Swagelok, SS 304L coated with a 0.001" PTFE) for mass balance measurement of residual water saturation as well as elemental analysis by ICP spectroscopy.

Pressure measurements and instrument calibration

Low-pressure measurements of fluids in the experimental system were made with 10 bar pressure transducers (HBM P3TCP, 0.1% full scale accuracy). High-pressure measurements were made with 200 bar pressure transducers (HBM P6A, 0.2% full-scale accuracy). Transducers were connected via 7-wire cables to a data acquisition computer (HBM MGC+, 18-bit accuracy), and a 1.25 hz Bessel filter was applied. Data was stored as the average of 128 independently measured data points to further decrease noise. Low-pressure transducers were simultaneously calibrated relative to a portable pressure calibrator (Druck DPI 605, 0.025% accuracy). High-pressure transducers were simultaneously calibrated with a primary standard dead weight calibrator (DH Instruments PG7000-AMH, 5 ppm mass accuracy). All calibrations were performed with a series of first increasing then decreasing pressures going to >95% of full scale. The pressure offset between transducers located before and after the core was corrected in each experiment by a linear fit between at least a pair of pressure offset measurements at pressures in the experimental range. All equipment was electronically monitored by a data acquisition computer (National Instruments) running a custom-written LabView VI capable of automatically gathering, processing, and analyzing all data in real time.

Permeability measurements

Brine permeability was measured at atmospheric pressure as well as at experimental pressure (100 bar). Permeability measurements were made by flowing brine at a series of first increasing then decreasing flow rates in evenly spaced increments, e.g. 0-3 mL/min in 0.5 mL/min increments, while limiting the highest flow rate to maintain a Reynolds number below 0.5 to ensure laminar flow (Scheidegger, 1974). At least three independent measurements of permeability were made and their average reported for each experiment. Effective radial stress was controlled to be 35 bars in both low- and high-pressure measurements. In several instances, post-experiment cores were vacuum-baked dry overnight, reloaded, evacuated of air overnight, and then liquid CO_2 was used to saturate the core sample. High-pressure (100 bar) liquid CO_2 permeability was measured, and in all cases, the previous brine permeability measurements were confirmed.

CO_2 flood experiments

At the beginning of each experiment, air was evacuated from the core overnight. The core was then saturated with brine and low- and high-pressure brine permeability was measured. CO_2 was then used to purge the system of brine up to just before the core holder via a bypass to minimize CO_2/brine mixing and carbonic acid formation before the core itself. CO_2 pressure was then built up to 100 bar and allowed to equilibrate for about an hour. CO_2 core flooding then began and proceeded in a series of incremental flow rates, with each increment occurring after the pressure drop across the core had stabilized. Flow rates were chosen so that each experiment lasted no longer than 3-4 hours, avoiding any significant diffusion-controlled evaporation of brine. The first flow rate was chosen based upon a Matlab code providing a numerical estimate of breakthrough time by assuming multiphase Darcy flow with a Brooks-Corey capillary pressure-saturation-relative permeability relationship (Sivakumar and Ramakrishnan, 2006). Flow was doubled to a reasonably high flow rate, typically around 10 mL/min, and then increased in linear steps until the system's maximum stable flow rate was achieved at approximately 30-50 mL/min (see Figures 3 and 4 below). We applied a measurement technique that was designed to correct for capillary end effects (Ramakrishnan and Capiello, 1991). Rather than fitting relative permeability to the ratio of flow rate to measured pressure drop across the

core (Equation 4), a slope is fitted between two data points at similar flow rates such that the capillary end effect should be identical in both (Equation 5).

$$k_r=(\mu \, L/k) \, Q/\Delta P \qquad \text{(Eq. 4)}$$

$$k_r=(\mu \, L/k) \, dQ/d\Delta P \qquad \text{(Eq. 5)}$$

Sources of measurement error

A source of error in the experiments is the potential for evaporation of brine into the unsaturated CO_2 phase. However, this would tend to overestimate the measured relative permeability as more flow pathways or more pore space allow greater CO_2 flow. Experimental data was noisy, varying by 5-10%, but not affecting the overall trends in the data. The back-pressure regulators are a source of error and were not able to tightly control pressure, resulting in pressure drifts and occasional pressure shifts on the order of a bar, contributing to noise. We conclude these errors do not significantly affect our primary conclusions.

Results

Experiments were conducted using samples of Berea sandstone and P3C alumina ceramic. Sample results are shown in Figures 3 and 4. Experimental conditions are noted in the figure captions. A summary of experimental conditions and results for representative experiments is shown in Table 1. The experiments universally had intermediate values of end point drainage CO_2 relative permeability (Table 1 below).

The first experiments were a P3C alumina ceramic (12.2 mD) and higher permeability Berea sandstones (688, 665 mD) with a 5% brine at liquid CO_2 conditions (100 bar, 20°C). To ensure that salt precipitation was not affecting this result, later experiments were repeated with reduced salt (1% NaCl) on a lower permeability Berea sandstone (119 mD).

17
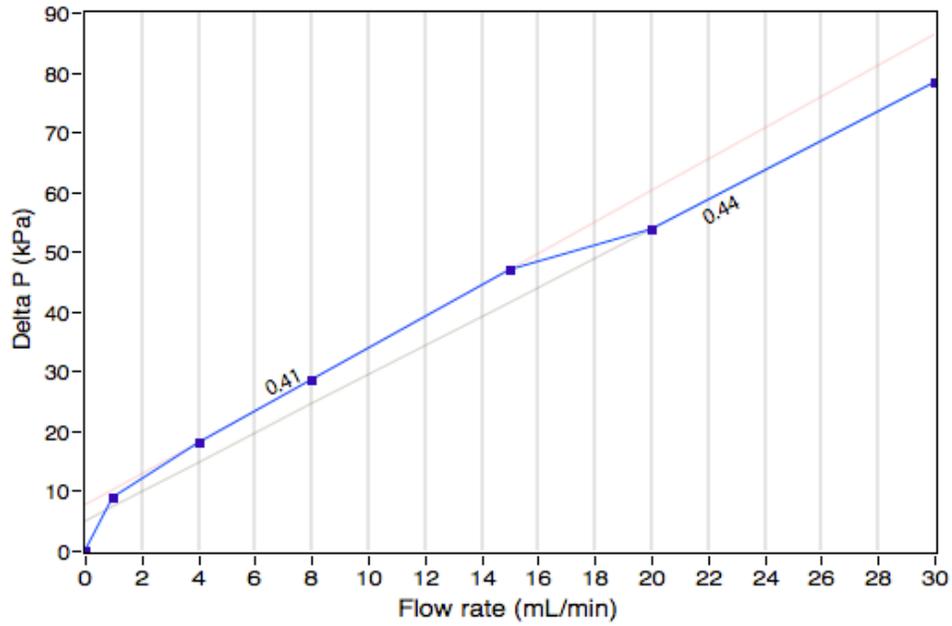
Figure 3: Sample results for relative permeability of CO_2 in Berea 100 sandstone core at 20 °C, 100 bar, 1% NaCl, k_{r_CO2}=0.44. The blue line plots the flow rate vs. pressure drop data. Slopes fit between adjacent data points provide the relative permeability, incorporating the capillary end effect. A drop in backpressure between 15 and 20 mL/min caused a subsequent decline in pressure drop, but the data is consistent on either side of this shift with k_{r_CO2}=0.41 between 4 and 15 mL/min and k_{r_CO2}=0.44 between 20 and 30 mL/min.
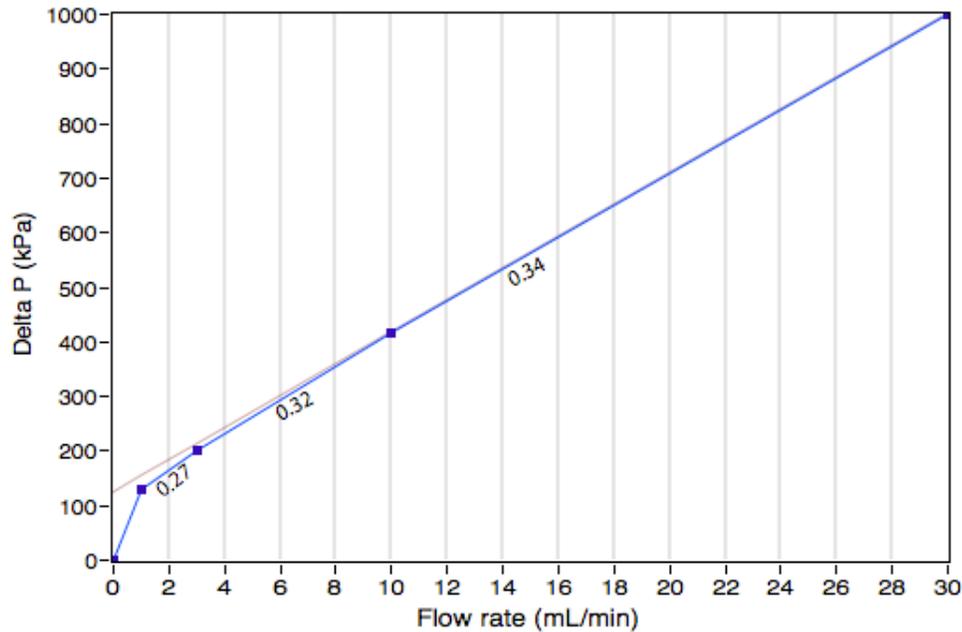
Figure 4: Sample results for relative permeability of CO_2 in P3C alumina ceramic core at 20°C, 100 bars, DI water, k_{r_CO2}=0.34. The blue line plots the flow rate vs. pressure drop data. The slope fit between adjacent data points provides the relative permeability, incorporating the capillary end effect.

Additional experiments were conducted with synthetic inert and homogeneous P3C alumina, and with deionized water in place of 5% brine to eliminate any possibility of permeability reduction due to physical rearrangement of the pore network. This was followed by several experiments at supercritical conditions (100 bar, 50°C) to ensure two-phase flow by moving far away from both the gas-liquid and liquid-hydrate transitions on the CO_2 phase diagram. Finally a set of experiments was performed with a modified setup at 20°C with varying back pressure including gas and liquid phase CO_2 (10, 20, 35, 65 bars), with similar results. In all cases, we found drainage end point relative permeability values (twelve experiments in total) to be tightly clustered, with seven experiments between 0.34-0.40, an additional three experiments in the range of 0.30-0.50, and two outlier measurements at values of 0.19 and 0.56. This result suggests that the conventional assumption of CO_2 having a relative permeability close to unity may be inappropriate.

Core	Endpoint CO_2 relative permeability	Average endpoint CO_2 saturation	Pressure (bars)	Temp (°C)	CO_2 phase	Brine	Porosity (%)
P3C	0.34	0.67	100	20	Liquid	5%	42.5
Berea	0.19	0.60	100	20	Liquid	5%	24.0
Berea	0.38	0.55	100	20	Liquid	5%	24.0
P3C	0.37	0.76	100	20	Liquid	DI	42.5
P3C	0.30	0.76	100	50	Supercritical	DI	42.5
P3C	0.34	0.66	100	20	Liquid	DI	42.5
Berea	0.44	0.95	100	20	Liquid	1%	15.7
P3C	0.37	0.60	100	50	Supercritical	DI	42.5
P3C	0.38	N/A	10	20	Gas	DI	42.5
P3C	0.40	N/A	20	20	Gas	DI	42.5
P3C	0.56	N/A	35	20	Gas	DI	42.5
P3C	0.50	N/A	65	20	Liquid	DI	42.5

Table 1: Summary of test samples, laboratory conditions, and experimental results for drainage end point relative permeability of CO_2 displacing water.

Discussion

Our results from these experiments show that CO_2 relative permeability is not indicative of a non-wetting fluid and therefore does not correspond to an inert gas, suggesting important interactions occur between CO_2 and water at a pore or molecular scale. Because the measured relative permeabilities are significantly lower than expected, carbon sequestration models will need to incorporate sensitivity to this parameter. We anticipate that this will have a major impact on capacity estimates for CO_2 storage in many potential reservoirs.

Prior to these flow-through reactor experiments, we anticipated that the drainage endpoint relative permeability of (inert) CO_2 displacing water would be in the range of 0.8-1. Instead, all of our experiments resulted in intermediate values for relative permeability of CO_2 displacing water, more typical of a weakly non-wetting to intermediate wetting fluid. Other recent investigations of the relative permeability of CO_2 displacing brine have also shown low CO_2 relative permeabilities supporting this conclusion, though with experimental designs that had not been focused on endpoint CO_2 relative permeability (Bachu and Bennion, 2008; Perrin and Benson, 2010).

These intermediate relative permeability values imply that CO_2 cannot be treated as an inert non-wetting phase. Experiments with CO_2 in silica aerogels, as well as molecular dynamics simulations between CO_2 and muscovite, have shown CO_2 layers bound to mineral surfaces (Cole et al., 2010). Contact angle measurements of saturated CO_2 and water on quartz and mica show an increasing contact angle as high as 60° through the water phase with increasing pressure (Chiquet et al., 2007). Although the molecular and pore scale physics and chemistry involved in this experiment remain unclear at this time, possible mechanisms for this include CO_2-rock interactions through carbonic acid formation, miscibility with subsequent fluid-rock interactions, or even complex CO_2-water-rock interactions.

Lower CO_2 relative permeability will affect the flow of CO_2 in both onshore and offshore reservoirs in several ways. Storage capacities will be decreased in pressure-limited reservoirs where storage capacities are determined by the caprock fracturing pressure. In tilted reservoirs, CO_2 plume areas scale as the square root of the mobility ratio $\sqrt{(\lambda_{CO2}/\lambda_{H2O})}$, where mobility is defined as $\lambda = k_r/\mu_r$ (Nordbotten and Celia, 2006). Therefore, storage capacities will increase in area-limited reservoirs where plume migration may be constrained. Furthermore, the intermediate value for CO_2 wettability found in this study supports concerns that higher CO_2 contact angles will decrease the capillary breakthrough pressure and allow leakage at lower pressures in certain reservoirs previously trapping natural gas. Also, a reduction in CO_2 mobility may stabilize plume fronts, as similar analyses have shown for water flooding in oil reservoirs (Willhite, 1986). A variety of indirect effects including plume evolution and residual capillary trapping may also be linked to mobility (Spiteri et al., 2005; Juanes and MacMinn, 2008).

Based on these results, modeling efforts should incorporate the sensitivity to varying relative permeability of CO_2 in brine-saturated formation (see, e.g., Burton et al., 2009). Additionally, future petrophysical analyses for potential CO_2 sequestration sites should include core-scale relative permeability measurements to improve the versatility of reservoir models. Similar core analyses are routinely conducted in the petroleum industry[2].

---

[2] This work will be published in the Proceedings of the 10th International Conference on Greenhouse Gas Control Technologies (Levine et al., 2011) and in greater detail in the Ph.D. dissertation of Jonathan Levine (Columbia University, 2010).

IV. Hydrate and Dissolution Experiments

Materials and Methods

High-pressure experimental testing for CO_2 injection into reactive formations (i.e. limestone or basalt) as well as the formation of hydrates is within the design specifications and capability of the Schlumberger core flooding system described in Section II. The system used to visualize hydraulic fracturing and buoyant fracture rise using transparent gelatin, laponite, and dyed fluids (described in Section I) could also be the basis of experiments testing the effects of hydrate formation on these processes. Such experiments had to be deferred within the scope of this project due to the unexpected, but critical, results discussed in Section II concerning the multiphase water-CO_2 transport experiments, and thus greater time and emphasis placed on them. Multiphase transport must be understood in the absence of reactive geochemistry, heterogeneity, and hydrate formation before being able to iteratively add each of these complexities. High-pressure core flooding experiments are planned for the future, incorporating each of these in a methodical manner and introducing one new variable at a time to evaluate the effects of heterogeneity, reactivity, and hydrate formation under reservoir conditions. Furthermore, the expertise developed by the doctoral student trained under this award will be pursuing further hydrate-related research at the Center for Hydrate Research at the Colorado School of Mines and its potential application to CO_2 injection into ocean sediments.

Discussion

The formation of CO_2 hydrate under in situ conditions relevant in marine sediments may significantly affect their potential for CO_2 injection and sequestration. For example, hydrate formation may cause permeability reductions (Kleinberg et al., 2005) and increase sediment strength at high saturations (Santamarina et al., 2004). However, hydrate formation may also be limited by low permeability in fine-grained, porous sediments. The kinetics of hydrate formation are also very fast (Sloan and Koh, 2007) and could be anticipated to overwhelm the time needed for fracture propagation, and would certainly be much faster than buoyant fracture rise (Nunn and Muelbroek, 2002). However, hydrates can only form in the presence of water and CO_2, and so might be transport-limited in low permeability sediments. Given the low relative miscibility of water and CO_2, it is likely the interface between water and liquid CO_2 will act as a self-limiting transport barrier, and as such, hydrate may remain as a stable skin with hydrate growth

controlled by slow diffusion across the barrier itself (Sloan and Koh, 2007). For CO_2-filled fractures, hydrate may be expected to form as a skin at the fracture boundary, reducing permeability and potentially preventing any further transport across its boundary, similar to proposed behavior of natural gas hydrate-filled fractures (e.g., Kleinberg, 2006; Cook et al., 2008). This behavior suggests that CO_2 actively injected into a vertically propagating fracture will not have sufficient water available for hydrate to form or arrest its propagation; however, slow-rising buoyant fractures may have sufficient water available for hydrate to form and deprive the fracture of the fluid volume and pressure necessary for buoyant rise.

V. Conclusions

The low permeability of pelagic sediments will require large injection areas that could be attained using extremely long horizontal wells, by hydraulic fracturing, or both. To safely fracture deep ocean sediments without a mechanical stress or strength barrier, a fracture arrest mechanism must be identified to stop both dynamic fracture growth and buoyant fracture rise toward the seafloor. Experiments with sediment and injection fluid proxies allow different fracture arrest mechanisms to be tested. These include artificial stress barriers or change fracture orientation, reservoir engineering additives such as an impermeable buoyant diverter or proppant, relying on CO_2 hydrate formation, or the combination of these different methods. By identifying a solution, reservoir simulations may be built to incorporate fracture dynamics and their potential arrest mechanisms. The results of such a simulation would allow evaluation of the flow rates and storage capacity of a potential CO_2 sequestration site in deep ocean sediments. Successful reservoir engineering in deep ocean sediments could enable CO_2 sequestration over potentially large regions of the ocean floor (Levine et al., 2007) and within close proximity to industrial CO_2 sources.

Endpoint relative permeability experiments of CO_2 displacing water from synthetic and natural rock cores at both liquid and supercritical conditions determine this critical parameter of a geological reservoir. Endpoint CO_2 relative permeability is shown to have intermediate values with the results tightly clustered around 0.4. We conclude that CO_2 cannot be treated as an inert non-wetting phase, and further pore-scale experiments are needed to explain the causal physics and chemistry of this result. Based on these results, pressure-limited reservoirs will have reduced capacity while area-limited reservoirs will have increased capacity. Modeling efforts are also

needed to incorporate the effect of reduced relative permeability, as well as the model's sensitivity to varying relative permeability values. Finally, because injectivity and storage capacity are highly sensitive to relative permeability, future petrophysical analyses for potential CO_2 sequestration sites should include relative permeability measurements on reservoir core samples rather than relying on extrapolations based on prior studies.

References

Anderson, W., "Wettability Literature Survey Part 5: The Effects Of Wettability On Relative Permeability," *Journal of Petroleum Technology,* vol. 39, no. 11, pp. 1453–1468, 1987.

Bachu, S., and B. Bennion, "Effects of in-situ conditions on relative permeability characteristics of CO2-brine systems," *Environmental Geology,* vol. 54, no. 8, pp. 1707–1722, 2008.

Bakala, M., Fracture propagation in sediment-like materials, M.S. thesis, 83 pp., Univ. of Oklahoma, OK, 1997.

Barree, R.D., and H. Mukherjee, Design Guidelines for Artificial Barrier Placement and Their Impact on Fracture Geometry*, Soc. Pet. Eng. SPE* 29501-MS, 1995.

Bielicki, J., "The Viability of Permanent Carbon Capture and Storage in Deep Sea Sediment," *EOS Transactions*, AGU. 88(52), Fall Meeting Supplement, Abstract U42A-04, 2007.

Burton, M., N. Kumar, and S. Bryant, "CO2 injectivity into brine aquifers: Why relative permeability matters as much as absolute permeability," *Energy Procedia,* vol. 1, no. 1, pp. 3091–3098, 2009.

Chiquet, P., D. Broseta, and S. Thibeau, "Wettability alteration of caprock minerals by carbon dioxide," *Geofluids,* vol. 7, no. 2, pp. 112–122, 2007.

Cole, D.R., A.A. Chialvo, G. Rother, L. Vlcek, and P. T. Cummings, "Supercritical fluid behavior at nanoscale interfaces: Implications for CO2 sequestration in geologic formations," *Philosophical Magazine,* vol. 90, no. 17, pp. 2339–2363, 2010.

Cook, A., D. Goldberg, and R. Kleinberg, "Fracture-controlled gas hydrate systems in the northern Gulf of Mexico," *J. Mar and Petrol Geol.,* doi:10.1016/j.marpetgeo.2008.01.013.

Donaldson, E., N. Ewall, and B. Singh, "Characteristics of capillary pressure curves," *J. Petrol. Sci. and Eng.,* vol. 6, no. 3, pp. 249–261, 1991.

Gudmundsson, A., and S.L. Brenner, "How hydrofractures become arrested," *Terra Nova* 13 (6), 456–462 doi:10.1046/j.1365-3121, 2001.

House, K. Z., D.P. Schrag, C.F. Harvey. and K.S. Lackner, "Permanent carbon dioxide storage in deep-sea sediments," *PNAS*, 103(33), 12291-12295, 2006.

Hubbert, M.K., and D.G. Willis, "Mechanics of hydraulic fracturing," *J. Pet. Technol.*, 9, 153–168, 1957.

IPCC, IPCC Special Report on Carbon Dioxide Capture and Storage. IPCC, 2005.

IPCC, "The physical science basis," Contribution of Working Group I to the Fourth Assessment Report of the Intergovernmental Panel on Climate Change, 2007.

Juanes, R., and C. W. MacMinn. Upscaling of capillary trapping under gravity override: application to CO2 sequestration in aquifers. In SPE/DOE Symposium on Improved Oil Recovery, number SPE 113496, Tulsa OK, USA, 2008. *Society of Petroleum Engineers*.

Kleinberg, R.L., C. Flaum, and T.S. Collett, "Magnetic resonance log of Mallik 5L38: Hydrate saturation, growth habit, and relative permeability", in S.R. Dallimore and T.S. Collett (Editors), Scientific Results from the Mallik 2002 Gas Hydrate Production Research Well, Mackenzie Delta, Northwest Territories, Canada, Bulletin 585. *Geological Survey of Canada*, Ottawa, 2005.

Kleinberg, R.L., "New Deposit Accumulation Model for Marine Gas Hydrates," *Offshore Technology Conference* OTC-18246, Houston, Texas, U.S.A., 1–4 May 2006.

Levine, J. S., J. M. Matter, D. Goldberg, A. Cook, and K.S. Lackner, "Gravitational trapping of carbon dioxide in deep sea sediments: Permeability, buoyancy, and geomechanical analysis," *Geophys. Res. Lett.,* 34, L24703, doi:10.1029/2007GL031560, 2007.

Levine, J. S., J. M. Matter, D. Goldberg, and K.S. Lackner, "Gravitational trapping of carbon dioxide in deep ocean sediments: hydraulic fracturing and mechanical stability," in the Proceedings of the 9th International Conference on Greenhouse Gas Control Technologies (GHGT 9), Washington D.C., November 16-20, 2008, in *Energy Procedia*, Vol.1, 3647-3654, http://dx.doi.org/10.1016/j.egypro.2009.02.161}{doi:10.1016/j.egypro.2009.02.16.

Levine, J. S., J. M. Matter, D.G. Goldberg, K.S. Lackner, M.G. Supp, and T.S. Ramakrishnan, "Two phase brine-CO2 flow experiments in synthetic and natural media," in the Proceedings of the 10th International Conference on Greenhouse Gas Control Technologies (GHGT 10), Amsterdam, The Netherlands, *Energy Procedia* (in press).

Levine, J., Relative permeability experiments of carbon dioxide displacing water and their implications for carbon sequestration. Ph.D. thesis, Columbia University, 2010.

Nguyen, H.X., and D.B. Larson, "Fracture height containment by creating an artificial barrier with a new additive," *Soc. Pet. Eng. AIME*, SPE 12061; SPE annual technical conference; 5 Oct 1983; San Francisco, CA, USA, 1983.

Nordbotten, J., and M. Celia, "Similarity solutions for fluid injection into confined aquifers," *Journal of Fluid Mechanics,* vol. 561, pp. 307–327, 2006.

Nunn, J.A., and P. Meulbroek, Kilometer-scale upward migration of hydrocarbons in geopressured sediments by buoyancy-driven propagation of methane-filled fractures, *AAPG Bulletin,* 86(5): 907-918, 2002.

Parhsall, J., "Barnett Shale Showcases Tight-Gas Development," *J. Pet. Technol.,* 60(9), 48-55, 2008.

Perrin, J., and S. Benson, "An Experimental Study on the Influence of Sub-Core Scale Heterogeneities on CO2 Distribution in Reservoir Rocks," *Transport in porous media,* vol. 82, no. 1, pp. 93–109, 2010.

Ramakrishnan, T., and A. Cappiello, "A new technique to measure static and dynamic properties of a partially saturated porous medium," *Chemical engineering science,* vol. 46, no. 4, pp. 1157–1163, 1991.

Santamarina, J.C., F. Francisca, T.-S. Yun, J.-Y. Lee, A.I. Martin, and C. Ruppel, "Mechanical, thermal, and electrical properties of hydrate-bearing sediments", In: Proceedings of Gas Hydrates: Energy Resource Potential and Associated Geologic Hazards, *AAPG Hedberg Conference,* September 12–16, 2004. Vancouver, Canada, 2004.

Scheidegger, A., "The physics of flow through porous media," 1974.

Secor, D. T., Jr., and D.D. Pollard, "On the Stability of Open Hydraulic Fractures in the Earth's Crust," *Geophys. Res. Lett.,* 2(11), 510–513, 1975.

Simonson, E.R., A.S. Abou-Sayed, and R.J. Clifton, "Containment of massive hydraulic fractures," *SPE* J 18 (1), pp. 27–32 [SPE 6089], 1978.

Sivakumar, R., and T.S. Ramakrishnan, "Dynamics of inviscid wetting phase displacement in a relative permeability measurement," Technical report, *Schlumberger research report,* Schlumberger-Doll Research, 2006.

Sloan, E. D., Jr., and A.C. Koh, Clathrate Hydrates of Natural Gases, 3rd ed.; Taylor & Francis-CRC Press: Boca Raton, FL, 2007.

Spiteri, E., R. Juanes, M. Blunt, and F. Orr, "Relative-Permeability Hysteresis: Trapping Models and Application to Geological CO2 Sequestration," *SPE Annual Technical Conference and Exhibition,* 2005.

Takada, A., "Experimental study on propagation of liquid-filled crack in gelatin: Shape and velocity in hydrostatic stress condition," *J. Geophys. Res.,* 95(B6), 8471–8481, 1990.

Warpinski, N.R., and P.T. Branagan, "Altered Stress Fracturing," *J. Pet. Tech,* 990-997, Sept. 1989.

Willhite, G., Waterflooding. Society of Petroleum Engineers, Richardson, TX, 1986.

For information on other
NYSERDA reports, contact:

New York State Energy Research
and Development Authority
17 Columbia Circle
Albany, New York 12203-6399

toll free: 1 (866) NYSERDA
local: (518) 862-1090
fax: (518) 862-1091

info@nyserda.org
www.nyserda.org

Permanent CO$_2$ Sequestration in Ocean Sediments: Flow-Through Reactor Studies

March 2011